Ab initio calculations of the linear and nonlinear susceptibilities of N_2, O_2, and air in midinfrared laser pulses

Jeffrey M. Brown,[1,2] Arnaud Couairon,[2] and Mette B. Gaarde[1]

[1]*Department of Physics and Astronomy, Louisiana State University, Baton Rouge, LA 70803-4001, USA*

[2]*Centre de Physique Théorique, Ecole Polytechnique, CNRS, Université Paris-Saclay, Route de Saclay, F-91128 Palaiseau, France*

(Received 10 April 2018; published 26 June 2018)

We present first-principles calculations of the linear and nonlinear susceptibilities of N_2, O_2, and air in the midinfrared (MIR) wavelength regime from 1–4 μm. We extract the frequency-dependent susceptibilities from the full time-dependent dipole moment that is calculated using time-dependent density functional theory. We find good agreement with curves derived from experimental results for the linear susceptibility and with measurements for the nonlinear susceptibility up to 2.4 μm. We also find that the susceptibilities are insensitive to the laser intensity even in the strong field regime up to 5×10^{13} W/cm^2. Our results will allow accurate calculations of the long-distance propagation of intense midinfrared laser pulses in air.

DOI: 10.1103/PhysRevA.97.063421

I. INTRODUCTION

The propagation of ultrashort, intense laser pulses in gaseous media has been extensively studied in the visible and near-infrared wavelength regions [1]. The nonlinear optical phenomena associated with these pulses arise from a combination of the medium's linear optical properties (dispersion) and intensity-dependent nonlinear processes, such as Kerr self-focusing and ionization. With the new availability of ultrashort pulse laser sources in the midinfrared (MIR, 2–4 μm) we enter a new frontier in ultrafast science, where many applications in strong field physics benefit greatly from an increase of the quiver energy of the electron in the longer wavelength laser field [2]. However, there are still many open questions regarding the roles of various nonlinear processes that drive the long-range propagation of MIR pulses. It has been proposed that the relative influence of dispersion, self-focusing, and ionization may be different than those for near-infrared wavelengths [3]. Therefore, an accurate description of the linear and nonlinear optical properties of common gases in the atmosphere is crucial for predictive modeling of the long-range propagation of MIR laser pulses.

The linear optical properties of molecular nitrogen N_2 and molecular oxygen O_2 in the visible spectrum have been known since the 1960's [4–6] and have typically been modeled empirically in the visible region using Sellmeier-like equations. Newer measurements [7–9] have helped improve and extend the modeling up to 2 μm. The nonlinear optical properties of these species have also been measured [10,11] up to 2.4 μm. Of particular interest is the value of the nonlinear index coefficient n_2, where the total index of the medium n has a dependence on the instantaneous intensity of the laser I through relation $n = n_0 + n_2 I$. Experiments [12,13] and simulations [3] utilizing MIR laser wavelengths call for new investigations on the linear and nonlinear properties of the constituents of air above 2.4 μm.

Multiple theoretical approaches have been proposed for determining these optical properties. A Kramers-Krönig transformation of the multiphoton absorption rate led to the prediction of the dispersion of n_2 for noble gases in the midinfrared [14,15]. *Ab initio* multiconfiguration self-consistent field (MCSCF) cubic response theory calculations were performed to extract hyperpolarizability and subsequently the frequency dependence of n_2 for multi-ionized noble gases [16] and for N_2 [17]. Calculations of the nonlinear response of O_2 in the midinfrared seem to be relatively unexplored.

In this paper we calculate the linear and nonlinear optical properties of N_2 and O_2 molecules for wavelengths ranging from 1–4 μm. This is done using time-dependent density functional theory (TDDFT), as implemented in the software package OCTOPUS [18,19], to calculate the multielectron dipole response to a short, intense laser pulse. From the resulting dipole spectrum, it is possible to extract the linear and nonlinear optical properties of both gas species. We find that the extracted values for the linear index n_0 and nonlinear index n_2 of both species are independent of the laser intensities with the range 10^{10}–5×10^{13} W/cm^2 and that the values are in good agreement with published experimental data between 1–2.4 μm. We infer the linear and nonlinear optical properties of air from corresponding calculations for its constituents.

The outline of the paper is as follows. Section II details the calculation of the time-dependent dipole moment using TDDFT. Section III describes how the macroscopic linear and nonlinear susceptibilities are extracted from the microscopic time-dependent dipole moment. In Sec. IV the results of the calculated linear and nonlinear refractive indices are presented and compared to available experimental data, followed by a summary in Sec. V.

II. SIMULATIONS

We simulate the multielectron dynamics of N_2 and O_2 using TDDFT as implemented in the open source software package OCTOPUS [18]. Nonrelativistic Kohn-Sham density functional theory allows an interacting many-electron system to be represented by an auxiliary system of noninteracting electron densities where both systems have the same

ground-state charge density. The Hamiltonian of the noninteracting system is written as the sum of the kinetic energy operator T and the Kohn-Sham potential V_{KS}: $H = T + V_{\mathrm{KS}}[\rho(r,t)]$. The Kohn-Sham potential is a functional of the electron density ρ that is separated into $V_{\mathrm{KS}}[\rho] = V_{\mathrm{ext}} + V_{\mathrm{H}}[\rho] + V_{\mathrm{XC}}[\rho]$, where V_{ext} is the external potential arising from the nuclei and the laser field, V_{H} is the Hartree potential representing electrostatic interaction between electrons, and V_{XC} is the exchange-correlation operator that contains all nontrivial interactions. The exact form of V_{XC} is unknown and is therefore approximated to various levels of sophistication. For time-dependent calculations of the molecules interacting with the laser field, the adiabatic approximation is made and assumes that the exchange-correlation potential is time independent.

The simulations take place in two steps. The first is to determine the ground state through minimizing the total energy of the system. Convergence of the ground state energy to obtain a realistic value of the ionization potential I_p is important, since the energies of the high-lying occupied molecular orbitals determine much of the optical properties of the molecule. Once a suitable ground state has been found, the second step is a time-dependent calculation of the dipole moment of the total electronic response of the molecule as it interacts with the MIR laser pulse.

To achieve an accurate convergence to the ground state, each molecule requires a different set of simulation parameters. For the two molecular simulations, the default pseudopotentials provided with OCTOPUS are used and both molecules live on a cylindrical grid with dimensions length = 30, radius = 15, and a grid spacing = 0.3 (atomic units are used throughout unless otherwise specified). The grid spacing is such that the ground-state energy is converged, using convergence criterion parameter `ConvRelDens = 1e-7`, which in our calculations also leads to the convergence of the dipole spectrum in the region of interest. The large length is necessary to avoid boundary effects since long wavelength pulses can accelerate the electrons far from the origin during the time-dependent portion of the simulation [2,20]. Since only the lower-order harmonic response is needed for calculating the first- and third-order susceptibilities of the medium, the simulation parameters are chosen such that the dipole spectrum is converged up to and including harmonic 7.

For N_2 it is sufficient to run OCTOPUS simulations in spin-unpolarized mode, which places two electrons in each orbital. This effectively forces the same energy on both spin-up and spin-down electrons, reducing the computational cost by half. For N_2, a bond length of 2.068 was found to minimize the total energy of the system. The exchange-correlation (XC) functionals in the local density approximation (LDA) [21–23] work quite well with the addition of the Average Density Self Interaction Correction (ADSIC) [24]. From this configuration, the ground-state orbital energies match closely to the experimentally measured ones [25] (Table I).

The ground state of O_2, commonly known as triplet oxygen, contains two unpaired, spin-up electrons occupying two π_g molecular orbitals. Therefore, it is necessary to run OCTOPUS in spin-polarized mode, where spin-up and spin-down electrons are placed in their own orbitals and allowed to evolve independently in energy.

TABLE I. N_2 molecular orbitals (MO), occupation numbers (Occ), and energies for experimental (Exp) and calculated (Sim) values (atomic units).

MO	Occ	Exp	Sim
$2\sigma_g$	2	1.533	1.299
$2\sigma_u$	2	0.7717	0.7029
$1\pi_u$	4	0.6273	0.6760
$3\sigma_g$	2	0.5726	0.5953

For O_2, a bond length of 2.2866 was found to minimize the energy of the system. Using the GGA exchange-correlation functionals (`XCFunctional = gga_x_lb + gga_c_tca`) [26,27], we find good agreement between the calculated and measured orbital energies [28] (Table II). A number of other exchange-correlation functionals with varying levels of complexity were explored, including LDA and hybrid functionals ([box]3lyp, PBE0, M05), but none of these other options produced a ground state with an ionization potential I_p within 15% of the measured value.

For the time-dependent calculation, we calculate the response to a few-cycle, linearly polarized, MIR laser pulse given by

$$E(t) = E_0 \sin^{10}(\omega t/2N_c)\sin(\omega t)\,, \tag{1}$$

where the field strength $E_0 = \sqrt{2I_0/\epsilon_0 c}$ varies through the peak intensities $I_0 = 10^{10} - 10^{14}\,\mathrm{W/cm^2}$, $N_c = 8$ roughly corresponding to 1.5–2 cycles under the envelope, and $\omega = 2\pi c/\lambda$ with wavelengths λ corresponding to 1–4 μm. To minimize artifacts from portions of the electron density nearing the edges of the computational box, a complex absorbing potential (CAP) is added using the following parameters: `AbsorbingBoundaries = cap`, `ABWidth = 3`, and `ABCapHeight = -0.2`. The maximum ionization yield over the range of intensities and wavelengths in this work is on the order of 10^{-5}. This value is calculated from the final value of the electron density which decreases due to absorption of electron density that reaches the edge of the computational domain. The method of time propagation is approximated enforced time-reversal symmetry (`TDPropagator = aetrs`) with a step size of `dt = 0.04`. A $\sin^2$ window is applied to the end of time-dependent dipole moment to facilitate calculation of the spectrum.

TABLE II. O_2 molecular orbitals (MO), occupation numbers (Occ), and energies for experimental (Exp) and calculated (Sim, spin-up and spin-down) values (atomic units).

MO	Occ	Exp	Sim (up, dn)
$2\sigma_g$	2	1.697	1.452, 1.387
$2\sigma_u$	2	1.096	0.9445, 0.8770
$1\pi_u$	4	0.7218	0.7323, 0.6664
$3\sigma_g$	2	0.7273	0.7252, 0.6658
$1\pi_g$	2	0.4436	0.4688, 0.3966

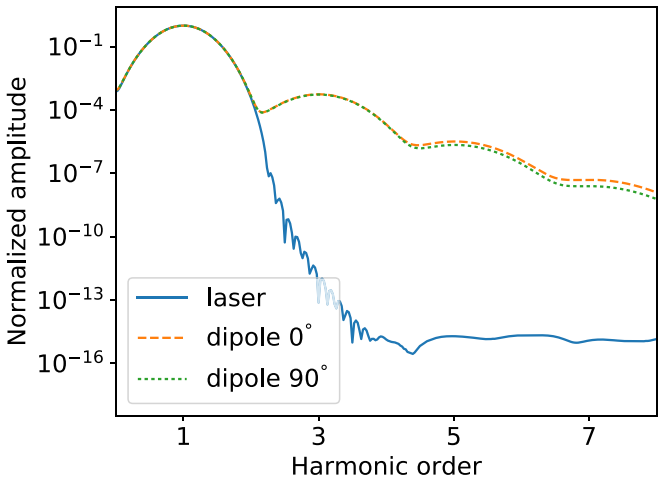

FIG. 1. The spectral amplitude of the laser pulse and the induced dipole moment of an N_2 molecule for two molecular orientations. 0° indicates that the polarization of the laser is aligned along the molecular axis, while for 90° they are perpendicular.

III. CALCULATION OF SUSCEPTIBILITIES

The goal of the time-dependent calculations is to extract the susceptibility of a bulk gaseous medium containing an ensemble of randomly oriented molecules. Therefore time-dependent simulations are performed for many angles $\theta = [0°, 15°, 30°, \ldots, 90°]$ between the molecular axis and laser polarization. The dipole spectra are calculated using the Fourier transform of the time-dependent dipole moments (Fig. 1).

The resulting magnitude of the dipole spectra at the fundamental laser frequency is found to have a $\cos^2(\theta)$ dependence even at a peak laser intensity of $I_0 = 10^{14}$ W/cm^2. Given the $\cos^2(\theta)$ dependence, it is possible to compute the polarization spectrum of an ensemble of randomly oriented molecules using a linear combination of the dipole spectra for parallel and perpendicular orientations of the molecules

$$\hat{P}(\omega) = \rho\left(\tfrac{1}{3}\hat{d}_{\parallel}(\omega) + \tfrac{2}{3}\hat{d}_{\perp}(\omega)\right), \tag{2}$$

where ρ is the neutral density of molecules. For N_2, $\rho = 2.688 \times 10^{25}$ m^{-3} and for $O_2 \rho = 2.505 \times 10^{25}$ m^{-3} at atmospheric pressure and room temperature. We note that this linear combination is typically valid only in the limit of low intensity laser pulses [29]. However, due to the low amount of ionization (a ground-state population reduction of $\approx 10^{-5}$) that occurs for midinfrared pulses even up to 10^{14} W/cm^2, we find that Eq. (2) is a good approximation.

The total susceptibility of the media, which includes both linear and nonlinear components, can be calculated by dividing the full polarization response spectrum $\hat{P}(\omega)$ by the laser's spectrum $E(\omega)$:

$$\chi(\omega) = \frac{\hat{P}(\omega)}{\epsilon_0 \hat{E}(\omega)}. \tag{3}$$

To extract the components of $\chi(\omega)$ corresponding to the linear $\chi^{(1)}(\omega)$ and nonlinear $\chi^{(3)}(\omega)$ properties of the medium, we employ a procedure that separates the linear and nonlinear responses spectrally.

In laser pulse propagation simulations the time-dependent polarization $P(t)$ of the medium is calculated as a power series expansion of odd harmonics of the field $E(t)$. For example, considering up to fifth-order nonlinear processes, the polarization is

$$P(t) = \epsilon_0[\chi^{(1)}E(t) + \chi^{(3)}E^3(t) + \chi^{(5)}E^5(t)]. \tag{4}$$

We relate the expansion Eq. (4) to the various harmonics in the dipole spectrum using the Fourier transform, yielding a set of equations where each polarization spectra $\hat{P}(n\omega)$ can be written as a sum of linear and nonlinear contributions up to order $\chi^{(5)}$:

$$\begin{aligned}\frac{1}{\epsilon_0}&[\hat{P}(\omega) + \hat{P}(3\omega) + \hat{P}(5\omega)] \\ &= \chi^{(1)}\hat{E}_1(\omega) + \chi^{(3)}\hat{E}_3(\omega) + \chi^{(5)}\hat{E}_5(\omega) \\ &\quad + \cancel{\chi^{(1)}\hat{E}_1(3\omega)} + \chi^{(3)}\hat{E}_3(3\omega) + \chi^{(5)}\hat{E}_5(3\omega) \\ &\quad + \cancel{\chi^{(1)}\hat{E}_1(5\omega)} + \cancel{\chi^{(3)}\hat{E}_3(5\omega)} + \chi^{(5)}\hat{E}_5(5\omega),\end{aligned}$$

where the quantities $\hat{E}_n(\omega)$ represent the Fourier transform of powers of the field $E^n(t)$. Terms containing no signal at a particular frequency are set to zero; for example, there is no third harmonic in the fundamental field and therefore $E_1(3\omega) = 0$. Collecting terms of the same harmonic order yields a set of equations where the frequency dependent susceptibility of each order can be written in terms of the calculated molecular polarizations P and field spectra E:

$$\chi^{(5)}(\omega) = \frac{\hat{P}(5\omega)}{\epsilon_0 \hat{E}_5(5\omega)}, \tag{5}$$

$$\chi^{(3)}(\omega) = \frac{\hat{P}(3\omega)}{\epsilon_0 \hat{E}_3(3\omega)} - \chi^{(5)}\frac{\hat{E}_5(3\omega)}{\hat{E}_3(3\omega)}, \tag{6}$$

$$\chi^{(1)}(\omega) = \frac{\hat{P}(\omega)}{\epsilon_0 \hat{E}_1(\omega)} - \chi^{(3)}\frac{\hat{E}_3(\omega)}{\hat{E}_1(\omega)} - \chi^{(5)}\frac{\hat{E}_5(\omega)}{\hat{E}_1(\omega)}. \tag{7}$$

Since these susceptibilities result from a time-dependent interaction between the molecules and a short laser pulse, they are generally valid for a range of frequencies near the central frequency. We will demonstrate this in more detail in the results section.

Conceptually, the subtraction procedure in Eqs. (5) to (7) corresponds to, for example, eliminating the contribution to the third harmonic yield from the fifth-order process that involves absorbing four laser photons and emitting one, and so on. The procedure is general and does not depend on the particular shape of the field $E(t)$ because the resulting spectral shape $E(\omega)$ is divided away in calculating the susceptibilities. It also avoids division by small values since the polarization at each harmonic order is divided by a spectral field component that also contains a signal at that particular harmonic. However, we note that this perturbative approach is limited to intensity and wavelength regimes where ionization is small.

In practice, it is only necessary to consider nonlinear processes up to $\chi^{(5)}$ to extract intensity-independent values for $\chi^{(1)}$ and $\chi^{(3)}$. The magnitude of the nonlinear contribution to the fundamental and third harmonic polarizations drops off quite rapidly as the harmonic order increases and becomes negligible for harmonic orders of 7 and above. We obtain intensity-independent susceptibilities over the wavelength

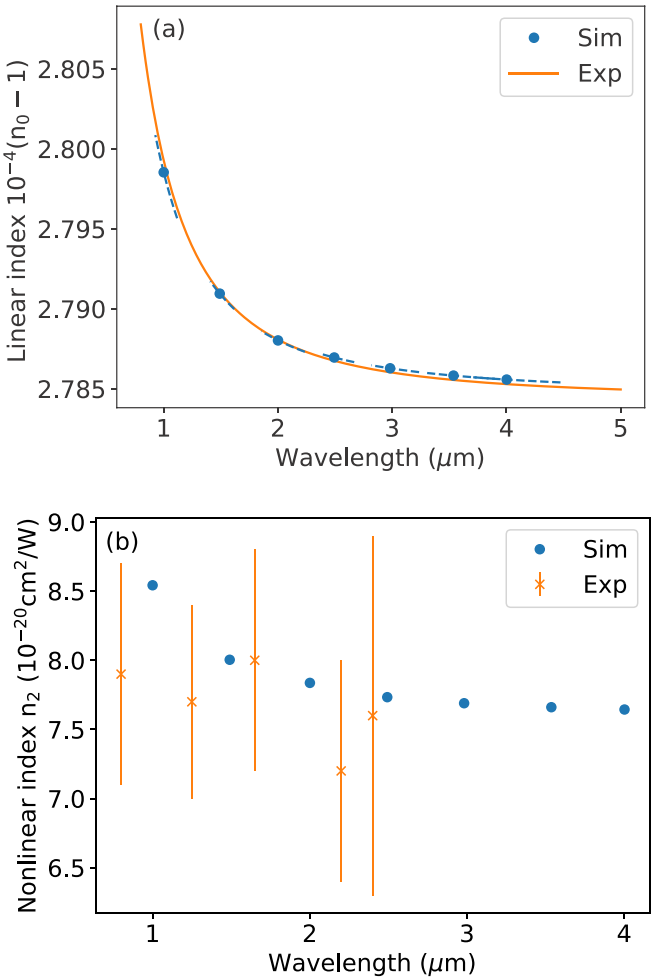

FIG. 2. The calculated (Sim) optical properties of N_2 compared to experimental values (Exp). (a) The calculated index of refraction n_0 is compared to the curve Eq. (10). (b) The nonlinear refractive index n_2 compared to experimental data [11].

range of 2–4 μm for peak intensities up to 10^{14} W/cm^2. For wavelengths between 1–2 μm, the extracted $\chi^{(3)}$ begins to show a small intensity dependence for peak intensity values above 5×10^{13} W/cm^2 due to a nonnegligible amount of ionization. Intensity limitations of a perturbative approach of modeling the total susceptibility of a medium has also been observed in *ab initio* calculations of atomic hydrogen [30].

Using the expressions for susceptibility in Eqs. (5) to (7), the linear refractive index is

$$n_0(\omega) = \sqrt{1 + \alpha \chi^{(1)}(\omega)}\,, \tag{8}$$

where α is a scaling factor described in more detail below. The nonlinear refractive index is

$$n_2(\omega) = \frac{3}{4} \frac{\chi^{(3)}(\omega)}{\epsilon_0 c n_0^2(\omega)}\,. \tag{9}$$

The scaling factor α ($\alpha = 1.055$ for N_2 and $\alpha = 1.034$ for O_2) is included to facilitate graphical comparison between the calculated values of this work and experimental values. The percentage adjustment of the linear susceptibility is consistent with the percentage difference between the calculated and measured values of I_p for both species, $\Delta I_p^{\{N_2\}} = 3.9\%$ and $\Delta I_p^{\{O_2\}} = 5.7\%$, where the simulations overestimated the binding energy of the highest energy electrons, resulting in a weaker response to the laser field. All values of the linear and nonlinear index that appear in this work contain the scaling factor α as described in Eqs. (8) and (9).

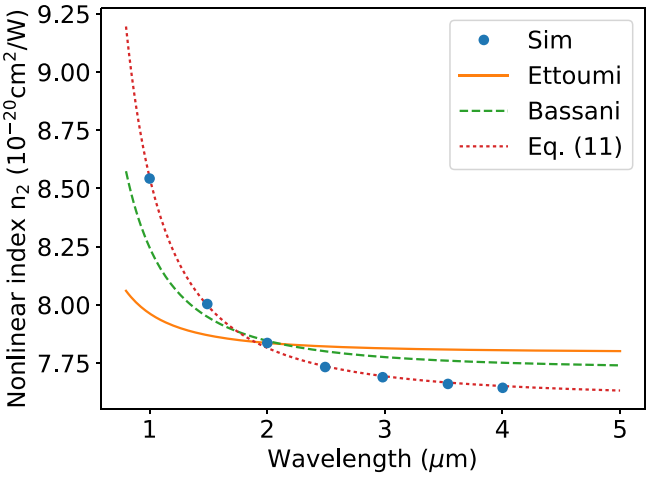

FIG. 3. The calculated (Sim) nonlinear refractive index values n_2 of N_2 are compared to two formulations of a generalized Miller's rule for third-order susceptibilities. The best match for these values if obtained by the Sellmeier-like equation (11).

IV. RESULTS

In Fig. 2(a), the calculated values of the linear index n_0 for N_2 are compared to the curve derived from experimental data [4]

$$n(\lambda) = 1 + 6.497378 \times 10^{-5} + \frac{3.0738649 \times 10^{-2}}{\lambda_0^{-2} - \lambda^{-2}}\,, \tag{10}$$

where $\lambda_0^{\{n_0,N_2\}} = 0.0833$ μm and is valid from 0.4679 to 2.0586 μm. Despite the stated upper limit of 2 μm, Eq. (10) fits the calculated values remarkably well up to 4 μm. The data points marked with dots are extracted from χ_1 evaluated at the central frequency of the laser pulse. The thin dashed lines extending from each data point shows the frequency dependence of the linear index, extracted from frequencies slightly above and below the central frequency. It is interesting to note that wavelength dependence extracted from each time-dependent calculation agrees with the overall wavelength dependence to within less than 0.1%.

In Fig. 2(b), the nonlinear index is compared to experimental data [11] and is also found to be in very close agreement. Since there is a decreasing spectral trend of the calculated values of n_2, it is interesting to compare its curve to the prediction provided by a generalized Miller's rule for third-order susceptibilities. Two formulations have been proposed in the literature. The first is $\chi^{(3)}(\omega) = \chi^{(3)}(\omega_0)[\chi^{(1)}(\omega)/\chi^{(1)}(\omega_0)]^4$ proposed by Ettoumi *et al.* [31] where ω_0 corresponds to a reference value (e.g., 2 μm). The second is $\chi^{(3)}(\omega) = \delta \chi^{(1)}(3\omega)\chi^{(1)}(\omega)^3$ proposed by Bassani *et al.* [32] where the factor $\delta = 2.841 \times 10^{-13}$ m^2/V^2 is determined by performing a least-squares fit

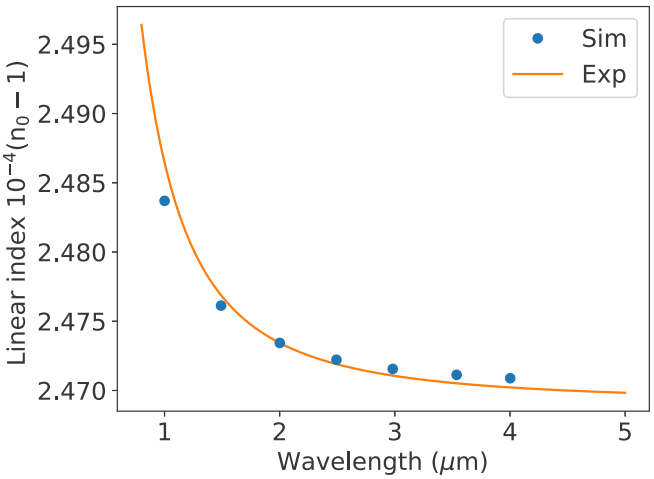

FIG. 4. The calculated values (Sim) of the index of refraction n_0 of O_2 are compared to the experimentally derived curve Eq. (12) (Exp).

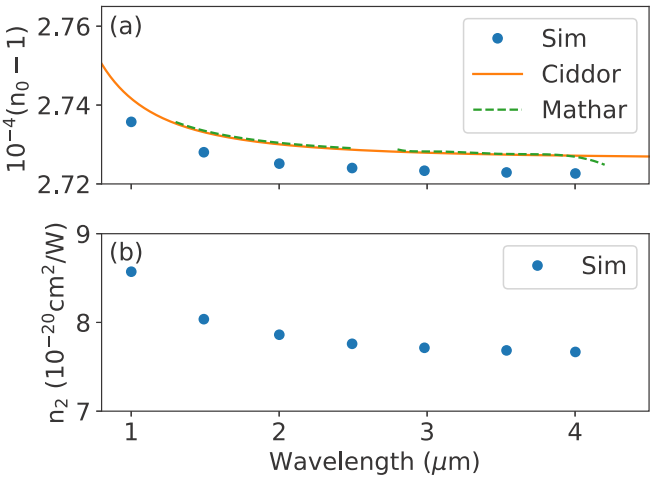

FIG. 6. (a) The calculated linear index values for air (Sim) are compared to the linear index curves of Ciddor 1996 [7] and of Mathar 2007 [34]. (b) The nonlinear index values n_2 of air using a proportional combination of values from N_2 and O_2.

of the simulation data. In Fig. 3, these predictive curves of n_2 are plotted along with the values calculated in this work.

It is clear that both predicted curves underestimate the dispersion of n_2 at long wavelengths compared to our calculated values since both are "flatter" at long wavelengths. This finding is consistent with that of the authors of Ref. [6] who pointed out that Miller's rule tends to underestimate the strength of the dispersion, and that there is not in general a strong correlation between the linear and nonlinear dispersion properties over a wide range of gases.

We find that the calculated values of n_2 are well fitted by a Sellmeier-like equation

$$n_2(\lambda) = \frac{P^{-1}}{\lambda_0^{-2} - \lambda^{-2}}\,, \tag{11}$$

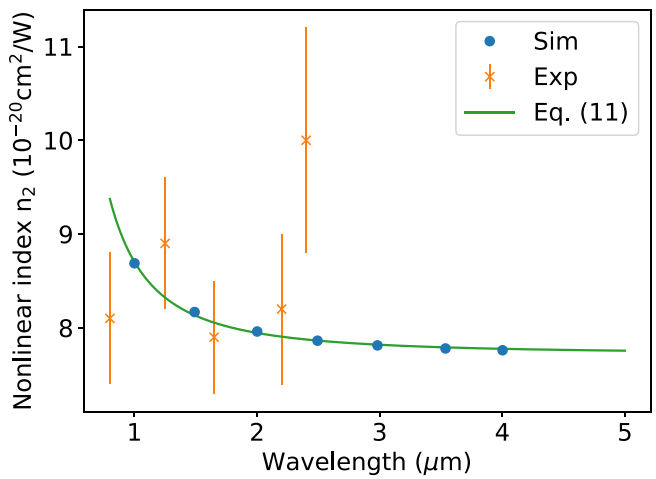

FIG. 5. The calculated values (Sim) for the nonlinear refractive index n_2 of O_2 are compared to measured values [11] (Exp) and to Eq. (11) with the appropriate parameters.

where $P^{\{N_2\}} = 14.63$ GW and $\lambda_0^{\{n_2,N_2\}} = 0.3334\ \mu$m. As seen in Fig. 3, Eq. (11) captures the dispersion of n_2 well, though it does force a singularity at $\lambda = 0.333\ \mu$m.

In Fig. 4, the calculated values for the linear index n_0 for O_2 are compared to the experimentally derived curve [8,9]

$$n(\lambda) = 1 + 1.181494 \times 10^{-4} + \frac{9.708931 \times 10^{-3}}{\lambda_0^{-2} - \lambda^{-2}}\,, \tag{12}$$

where $\lambda_0^{\{n_0,O_2\}} = 0.115\ \mu$m and is valid from 0.4 to 1.8 μm. Extending this curve into the midinfrared wavelength region shows that the scaled values of linear index from the simulation are well represented by Eq. (12). The calculated nonlinear index from the simulations is presented in Fig. 5 and is also in reasonable agreement with data from Shelton [11]. However, we do not find an increase of n_2 near 2.4 μm, which places our calculated values in closer agreement with the data from Shelton and Rice [33] for this particular wavelength. Just as with N_2, the values of n_2 for O_2 can be fitted with the Sellmeier-like equation (11) using the parameters $P^{\{O_2\}} = 14.62$ GW and $\lambda_0^{\{n_2,O_2\}} = 0.3360\ \mu$m.

We note that there is only a few percent difference between the calculated values of the nonlinear index n_2 for N_2 and O_2 and that this is merely a coincidence. In general, the value of I_p for a particular species is not necessarily correlated with its value of n_2. A well-known example of this is the case of Ar and N_2 which have very similar values of I_p, yet n_2 for Ar is roughly 25% larger than that of N_2 in the MIR regime [11].

A simple model for the optical properties of air can be constructed using a combination of the calculated susceptibilities for N_2 and O_2: $\chi^{(1)}_{air} = 0.8\chi^{(1)}_{N_2} + 0.2\chi^{(1)}_{O_2}$ and $\chi^{(3)}_{air} = 0.8\chi^{(3)}_{N_2} + 0.2\chi^{(3)}_{O_2}$. In Fig. 6(a), we compare the calculated values of $\chi^{(1)}_{air}$ to index curve Ciddor 1996 [7] (valid from 0.23–1.69 μm) and index curves Mathar 2007 [34] (valid in ranges 1.3–2.5 μm and 2.8–4.2 μm). We find remarkably good agreement and therefore we can recommend the use of these

curves for modeling the linear properties of air within the MIR wavelength regime of 1–4 μm. In Fig. 6(b), we plot calculated values of the nonlinear index for air and recommend the use of these values in simulations of the propagation of MIR laser pulses.

V. SUMMARY

Using *ab initio* calculations based on TDDFT, we calculate the linear and nonlinear refractive indices for N_2, O_2, and air for wavelengths of 1–4 μm. Close agreement between the experimental and calculated values of the linear index demonstrates that it is possible to extend the commonly used linear index curves into the MIR region without modification. We also find that the calculated nonlinear index values n_2 for N_2 and O_2 are in good agreement with experimental values up to 2.4 μm, and our calculations provide values for wavelengths up to 4 μm. We show that the predictive formulas for the nonlinear index using Miller's rule tend to underestimate the dispersion of n_2 at long wavelengths, and we propose an empirical, Sellmeier-type, fit instead.

Our results show that a fully time-dependent calculation of the molecular response to a strong field can be used to reliably extract linear and nonlinear susceptibilities for intensities up to $5 \times 10^{13}\,\mathrm{W/cm^2}$, as long as we correct for higher-order contributions to the dipole spectrum at a given frequency. Above $5 \times 10^{13}\,\mathrm{W/cm^2}$ the ionization-induced depletion of the ground state starts to influence the calculation and the extracted susceptibilities are no longer intensity-independent. Our results provide a benchmark for future experimental and theoretical determination of the linear and nonlinear refractive indices in the MIR spectral range, and will allow for accurate calculations of phenomena involving long-distance propagation in air.

ACKNOWLEDGMENTS

We acknowledge fruitful discussions with Paul Abanador, Ken Lopata, and Ken Schafer. This work was performed using the cluster computing facilities at Ecole Polytechnique (mésocentre PHYMATH). J.B. acknowledges support from the Air Force Office of Scientific Research under MURI Award No. FA9550-16-1-0013.

[1] A. Couairon and A. Mysyrowicz, Phys. Rep. **441**, 47 (2007).
[2] P. Agostini and L. F. DiMauro, Contemp. Phys. **49**, 179 (2008).
[3] P. Panagiotopoulos, P. Whalen, M. Kolesik, and J. Moloney, Nat. Photonics **9**, 543 (2015).
[4] E. R. Peck and B. N. Khanna, J. Opt. Soc. Am. **56**, 1059 (1966).
[5] E. R. Peck and K. Reeder, J. Opt. Soc. Am. **62**, 958 (1972).
[6] V. Mizrahi and D. P. Shelton, Phys. Rev. Lett. **55**, 696 (1985).
[7] P. E. Ciddor, Appl. Opt. **35**, 1566 (1996).
[8] J. Zhang, Z. H. Lu, and L. J. Wang, Appl. Opt. **47**, 3143 (2008).
[9] P. Křen, Appl. Opt. **50**, 6484 (2011).
[10] D. P. Shelton and J. E. Rice, Chem. Rev. **94**, 3 (1994).
[11] S. Zahedpour, J. K. Wahlstrand, and H. M. Milchberg, Opt. Lett. **40**, 5794 (2015).
[12] A. Mitrofanov *et al.*, Sci. Rep. **5**, 8368 (2015).
[13] N. A. Panov, D. E. Shipilo, V. A. Andreeva, O. G. Kosareva, A. M. Saletsky, H. Xu, and P. Polynkin, Phys. Rev. A **94**, 041801 (2016).
[14] C. Bree, A. Demircan, and G. Steinmeyer, IEEE J. Quantum Electron. **46**, 433 (2010).
[15] C. Brée, A. Demircan, and G. Steinmeyer, Phys. Rev. A **85**, 033806 (2012).
[16] M. Tarazkar, D. A. Romanov, and R. J. Levis, Phys. Rev. A **94**, 012514 (2016).
[17] M. Tarazkar, D. A. Romanov, and R. J. Levis, J. Phys. B **48**, 094019 (2015).
[18] X. Andrade, D. Strubbe, U. De Giovannini, A. H. Larsen, M. J. T. Oliveira, J. Alberdi-Rodriguez, A. Varas, I. Theophilou, N. Helbig, M. J. Verstraete, L. Stella, F. Nogueira, A. Aspuru-Guzik, A. Castro, M. A. L. Marques, and A. Rubio, Phys. Chem. Chem. Phys. **17**, 31371 (2015).
[19] X. Andrade, J. Alberdi-Rodriguez, D. A. Strubbe, M. J. T. Oliveira, F. Nogueira, A. Castro, J. Muguerza, A. Arruabarrena, S. G. Louie, A. Aspuru-Guzik, A. Rubio, and M. A. L. Marques, J. Phys.: Condens. Matter **24**, 233202 (2012).
[20] J. L. Krause, K. J. Schafer, and K. C. Kulander, Phys. Rev. A **45**, 4998 (1992).
[21] P. A. M. Dirac, Proc. Camb. Phil. Soc. **26**, 376 (1930).
[22] F. Bloch, Z. Phys. **57**, 545 (1929).
[23] J. P. Perdew and A. Zunger, Phys. Rev. B **23**, 5048 (1981).
[24] C. Legrand, E. Suraud, and P.-G. Reinhard, J. Phys. B **35**, 1115 (2002).
[25] "NIST electron-impact ionization cross sections", https://physics.nist.gov/cgi-bin/Ionization/table.pl?ionization=N2.
[26] R. van Leeuwen and E. J. Baerends, Phys. Rev. A **49**, 2421 (1994).
[27] V. Tognetti, P. Cortona, and C. Adamo, J. Chem. Phys. **128**, 034101 (2008).
[28] "NIST electron-impact ionization cross sections", https://physics.nist.gov/cgi-bin/Ionization/table.pl?ionization=O2.
[29] R. W. Boyd, in *Nonlinear Optics (Third Edition)*, edited by R. W. Boyd (Academic, Burlington, MA, 2008), pp. 253–275.
[30] A. Spott, A. Jaroń-Becker, and A. Becker, Phys. Rev. A **90**, 013426 (2014).
[31] W. Ettoumi, Y. Petit, J. Kasparian, and J.-P. Wolf, Opt. Express **18**, 6613 (2010).
[32] F. Bassani and V. Lucarini, Il Nuovo Cimento D **20**, 1117 (1998).
[33] P. Kaatz, E. A. Donley, and D. P. Shelton, J. Chem. Phys. **108**, 849 (1998).
[34] R. J. Mathar, J. Opt. A: Pure Appl. Opt. **9**, 470 (2007).